

## SAFETY DEMONSTRATION OF RPV UNDER PTS CONDITIONS USING CRUCIFORM TYPE SPECIMENS.

A. K. Pawar<sup>1</sup>, J. Chattopadhyay<sup>1</sup>, B. K. Dutta<sup>1</sup>, and K. K. Vaze<sup>1</sup>

<sup>1</sup>Scientific Officer, Bhabha Atomic Research Center, Mumbai, India (akpawar@barc.gov.in)

### ABSTRACT

Pre-test thermo-mechanical analyses using finite element method were carried out on four numbers of cruciform type specimens designed to simulate pressurized thermal shock (PTS) event in Reactor Pressure Vessel of PWR type reactors. The cruciform specimens were designed to produce different biaxial stress ratios 1:0, 1:1 and 2:1. Sequentially coupled thermal mechanical analysis approach was used to analyze the specimens. Biaxial mechanical stresses were produced in the core of the cruciform type specimen by subjecting the specimens to bending load and thermal stresses were produced in the specimens by heating the core of specimen to 300°C and then cooling it by spraying water. Various fracture mechanics parameters such as J-integral, crack mouth opening displacement (CMOD) and load line displacement (LLD) were evaluated. It is found that crack driving force (J-integral) increases during the thermal transient and crack growth is predicted in some of the specimens.

### INTRODUCTION

In the analysis of the structural integrity of Reactor Pressure Vessel (RPV) containing flaws, one of the important issues is the estimation of biaxial loading effect on fracture behavior of the material. This problem arises in connection with the normal operation of RPV as well as under the pressurized thermal shock loading. Figure 1 shows the typical flaw in a pressure vessel and the type of loading the flaw experiences. Figure 2 depicts the components of far field stress distribution in a RPV wall during a PTS transient.

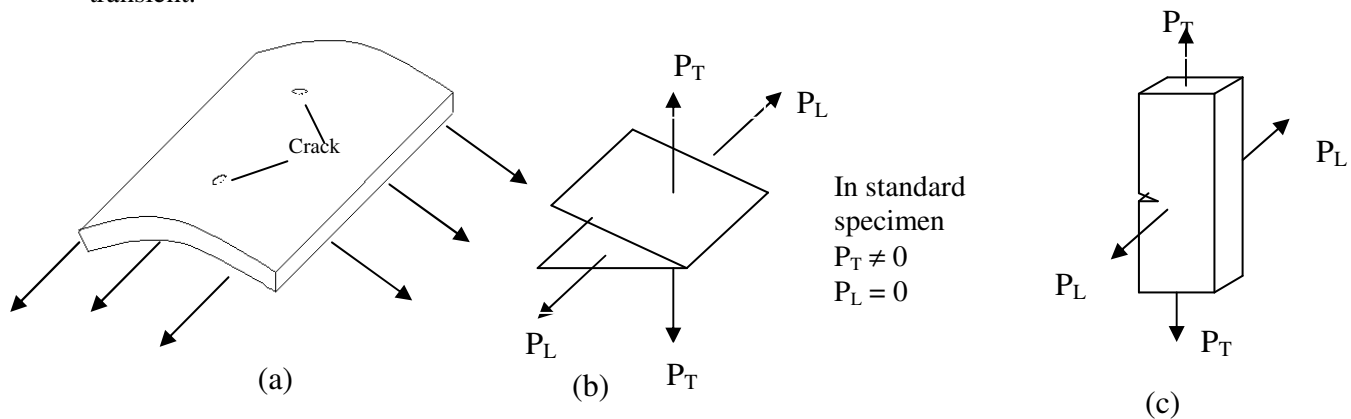
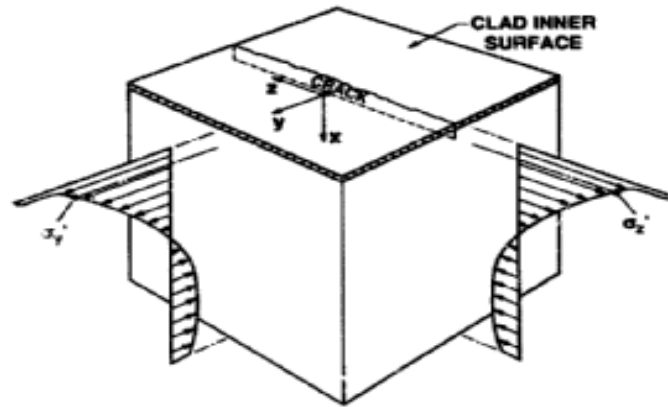
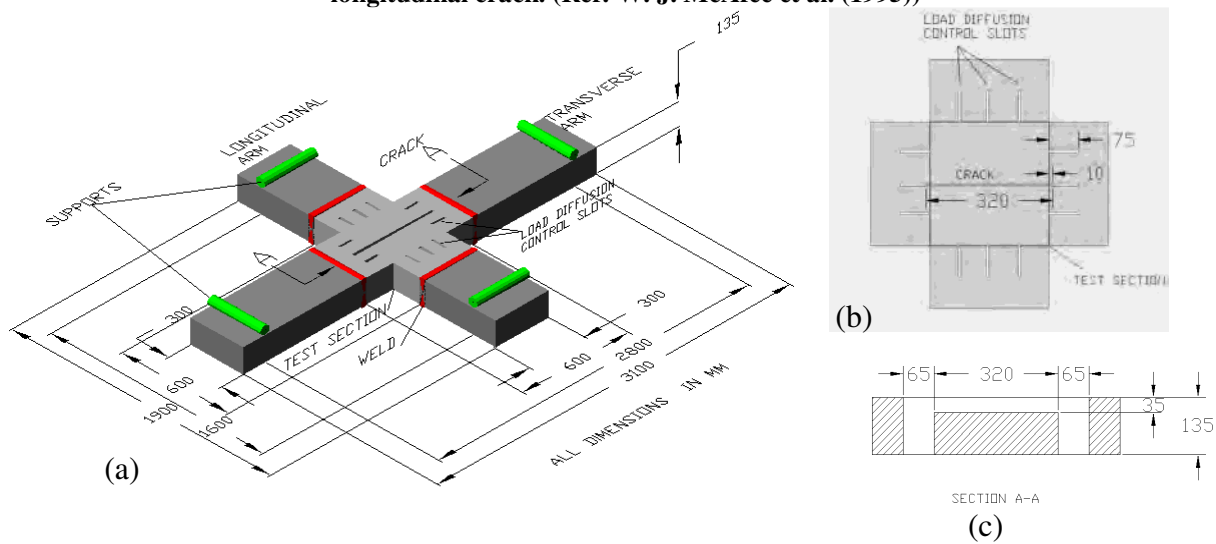


Figure 1 (a) Loading of pressure vessel. (b) Crack tip subjected to loading. (c) Typical specimen for fracture toughness

In the structural integrity analysis of RPV containing the flaws, the fracture toughness values obtained from standard laboratory specimens such as Compact Tension (CT), Three Point Bend Bar (TPBB) are normally used. These specimens are tested under in-plane opening mode (the load acts perpendicular to the crack front ( $P_T \neq 0$ ,  $P_L = 0$ , as in Figure 1 (c)). The out-of-plane loading ( $P_L$ ) is not represented in these specimens. There is growing interest worldwide to design a specimen, which can be tested to estimate the effect of biaxial loading on fracture behavior. The majority of the experiments on fracture toughness under biaxial loading have been performed on a plate subjected to biaxial bending moments (W. J. McAfee et al. (1995, 1996) and W. E. Pennell et al. (1995)).



**Figure 2 Vessel wall biaxial far-field stress during PTS transient with component aligned parallel to front of a longitudinal crack. (Ref: W. J. McAfee et al. (1995))**



**Figure 3 (a) Schematic of a cruciform specimen. (b) Specimen core. (c) Crack Geometry**

The configuration of the biaxial bend specimen having cruciform shaped geometry is depicted in Figure 3. The specimen design is capable of reproducing a linear approximation of the non-linear biaxial stress distribution in a RPV wall during a PTS transient (W. J. McAfee et al. (1995)). Reactor Safety Division (RSD), BARC has planned to carry out simulated pressurized thermal shock experiment using cruciform specimens to demonstrate the safety of reactor pressure vessel. Four cruciform specimens of different biaxiality ratio have been proposed to be tested under combined mechanical loading and thermal shock. Current paper deals with the pre-test analysis of these specimens. A brief description of the four specimens, which have been analyzed, is given below:

To simulate realistic scenario prevailing in a RPV under Loss of Cooling Accident (LOCA) condition, a cruciform specimen, CR21NOC, was designed to produce biaxial stresses in its core with biaxial stress ratio 2:1. The specimen is subjected to bending stresses such that state of stress in the specimen core is similar to that of the stresses prevailing in the RPV during Normal Operating Condition (NOC). Second specimen, CR10, was designed to produce uniaxial (biaxial stress ratio 1:0) stress in its core. The specimen was subjected to bending load till the onset of crack growth. Third cruciform specimen, CR11, was designed to produce biaxial state of stress across the crack in the core with biaxial stress ratio 1:1. The specimen was subjected to bending load till the onset of crack growth. The fourth cruciform specimen, CR21, has been designed to produce biaxial stresses across the crack in the core with biaxial stress ratio 10:1 in the elastic region. As the bending load increases, the longitudinal arms of the

specimen near the core start deforming plastically. Because of plastic deformation, transfer of some load occurs from longitudinal arms to transverse arms and the biaxial stress ratio changes. Ratio of span lengths for this specimen is kept such that biaxiality ratio reaches around 2:1 at the onset of the crack extension. In this way a state of biaxial stresses with a biaxial stress ratio 2:1 is ensured at the onset of crack-extension.

### GENERAL SPECIMEN GEOMETRY

Cruciform specimen consists of a core and arms. A solid model of the cruciform specimen is shown in Figure 3 (a). Specimen core is made of the same material as the reactor pressure vessel is i.e. 20MnMoNi55. Dimension of the core is 300x300x135 mm. Four 150 mm long projections are also part of the core made up of the same material. Figure 3 (b) shows the core of the specimen, which contains a crack, shown in Figure 3 (c). The crack is 320mm long and 35mm deep. Core has load diffusion control slots. An important concern in the design of cruciform specimen is that the crack-driving force should be uniform along the crack front with minimum values at the ends. This objective is achieved by introducing the slots in the specimen. These slots are instrumental in diffusing the stress along the crack-front and eliminating the stress concentration. Arms are welded to specimen core and are used to impart bending moment at the core. Arms are simply supported at the ends. Boiler Quality Carbon steel (ASTM-A-516

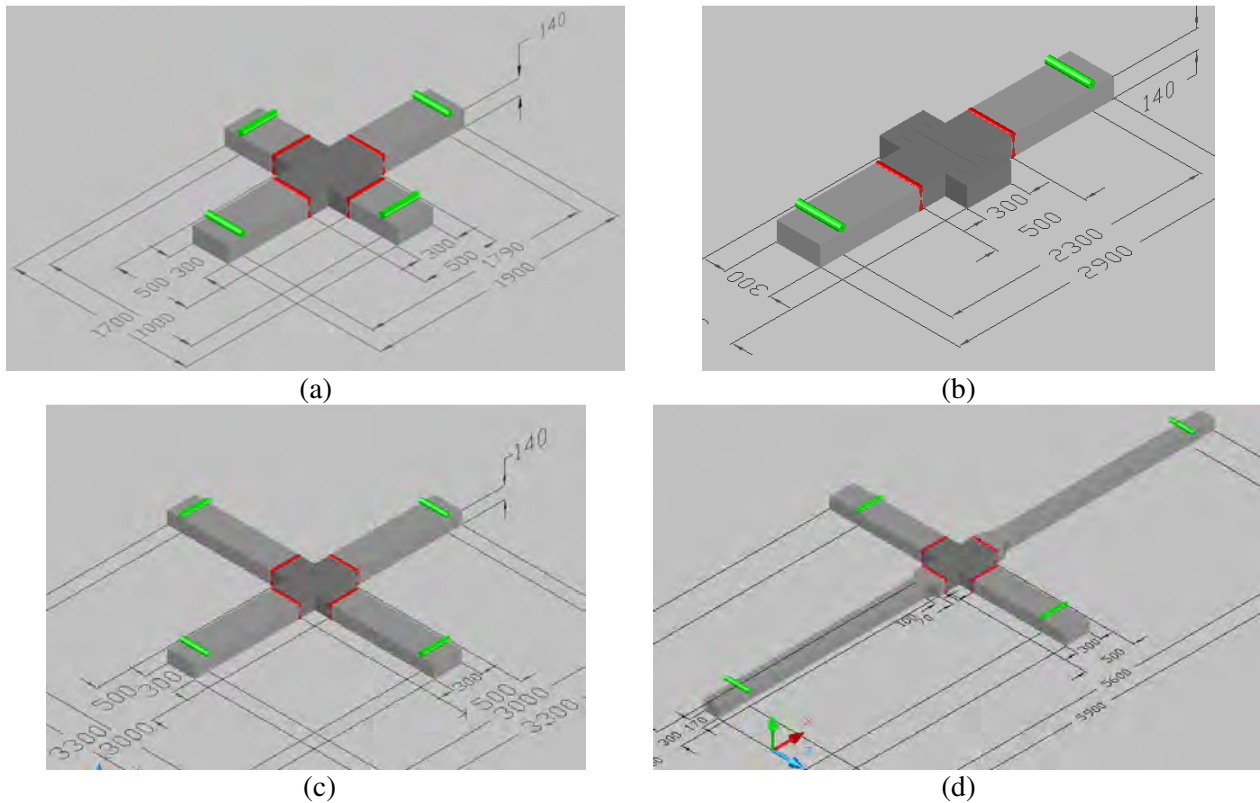


Figure 4 Cruciform specimens: (a) CR21NOC; (b) CR10; (c) CR11; (d) CR21.

Table 1 Dimensions of the cruciform specimens

Specimen Name	Length of transverse arm (mm)	Loading Span (mm)	Length of longitudinal arm (mm)	Loading Span (mm)	Test temperature	Biaxiality ratio	Crack length (mm)	Crack depth (mm)
CR21NOC	1700	1000	1900	1790	300°C	2:1	320	35
CR10	-	-	2800	2300	300°C	1:0	320	35
CR11	3300	3000	3300	3000	300°C	1:1	320	35
CR21	5900	5600	2800	2000	300°C	2:1	320	35

Grade 70) has been used to make the arms of the specimen. Specimen is subjected to load by a square load block at the center of the Core of the specimen opposite to the cracked face. Dimension of the load block is as 100x100 mm. A margin of 150 mm (overhang beyond the supports) on each side of the arms has been provided. Table 1 gives the dimensions of the four specimens proposed to be tested and Figure 4 (a-d) depict the four specimens.

### FINITE ELEMENT MODEL

Using the symmetry along two directions, one quarter of a specimen was modeled for finite element analysis. Solid model in Figure 5 (a) shows the scheme for analysis. Figure 5 (b-d) shows the mesh used for analysis at different zoom levels. Eight-node brick element was used for the analysis. Crack-front was modeled with a small radius of 0.2 mm making the crack-front blunt. Reduced integration was employed to eliminate the shear locking. The cruciform specimen was supported at the ends of its four arms. Load was applied on the specimen using a load block over the test section.

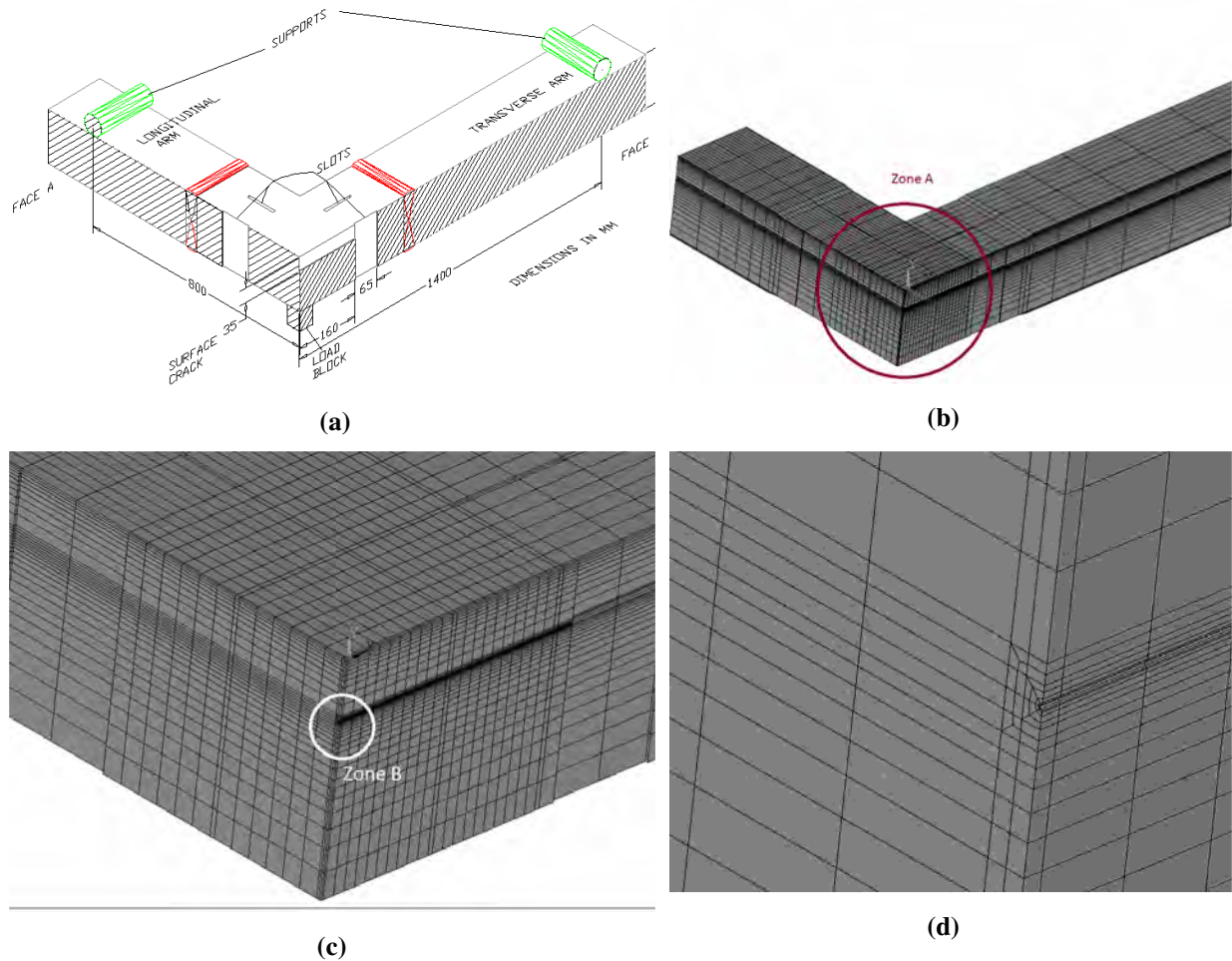
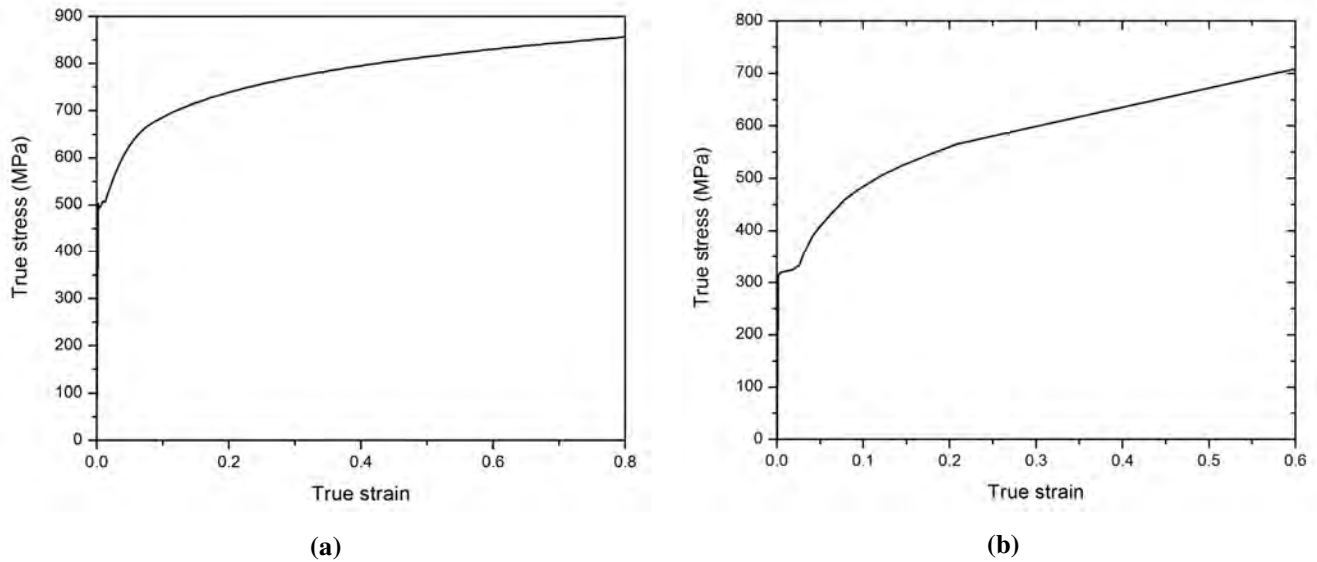


Figure 5 (a) One fourth section for FE Modeling; (b) Meshed Cruciform specimen; (c) Enlarged view of the cracked zone A of cruciform specimen; (d) Enlarged view of the cracked zone B of cruciform specimen

### MATERIAL PROPERTIES

The material used for the core of the cruciform specimen is 20MnMoNi55. The material properties of 20MnMoNi55 are: Young's modulus  $E = 210000$  MPa, Poisson's ratio  $\nu = 0.3$ . The yield strength of the material is 490.0 MPa. The stress strain curve for material is depicted in Figure 6(a). The material used for the arms of cruciform specimen is Boiler Quality Carbon steel conforming to ASTM SA 516 G-70. Material properties for this material are: Young's modulus  $E = 203000$  MPa, Poisson's ratio  $\nu$

= 0.3 and yield strength 312.0 MPa The true stress vs. true strain curve for the material is shown in Figure 6 (b). Thermal properties for 20MnMoNi55 and carbon steel are shown in Table 2 (Ref: KTA SAFETY STANDARD (1998)) and Table 3 (H.W. Schlapfer et al. (1990)) respectively.



**Figure 6 True stress vs true strain curve for: (a) 20MnMoNi55 material at room temperature; and (b) for carbon steel (ASTM SA 516 Gr-70) at room temperature.**

**Table 2 Thermal Properties of 20MnMoNi55**

	Temperature T °C			
	20	100	200	300
Thermal conductivity ( $Wm^{-1}K^{-1}$ )	44	44	43	41
Average linear thermal expansion coefficient between 20 °C and T ( $10^{-6}K^{-1}$ )	12.1	12.1	12.4	13.1
Average specific thermal capacity between 20 °C and T ( $kJ kg^{-1} K^{-1}$ )	12.1	0.46	0.49	0.51
Density ( $kg m^{-3}$ )	7860	7860	7860	7860

**Table 3 Thermal properties for the ASTM SA 516 Grade 70 carbon steel.**

	Temperature T °C			
	20	100	200	300
Thermal conductivity ( $Wm^{-1}K^{-1}$ )	51	50	48.34	46.1
Average linear thermal expansion coefficient between 20 °C and T ( $10^{-6}K^{-1}$ )	13.806	13.806	13.806	13.806
Average specific thermal capacity between 20 °C and T ( $kJ kg^{-1} K^{-1}$ )	0.48	0.48	0.53	0.57
Density ( $kg m^{-3}$ )	7860	7860	7860	7860



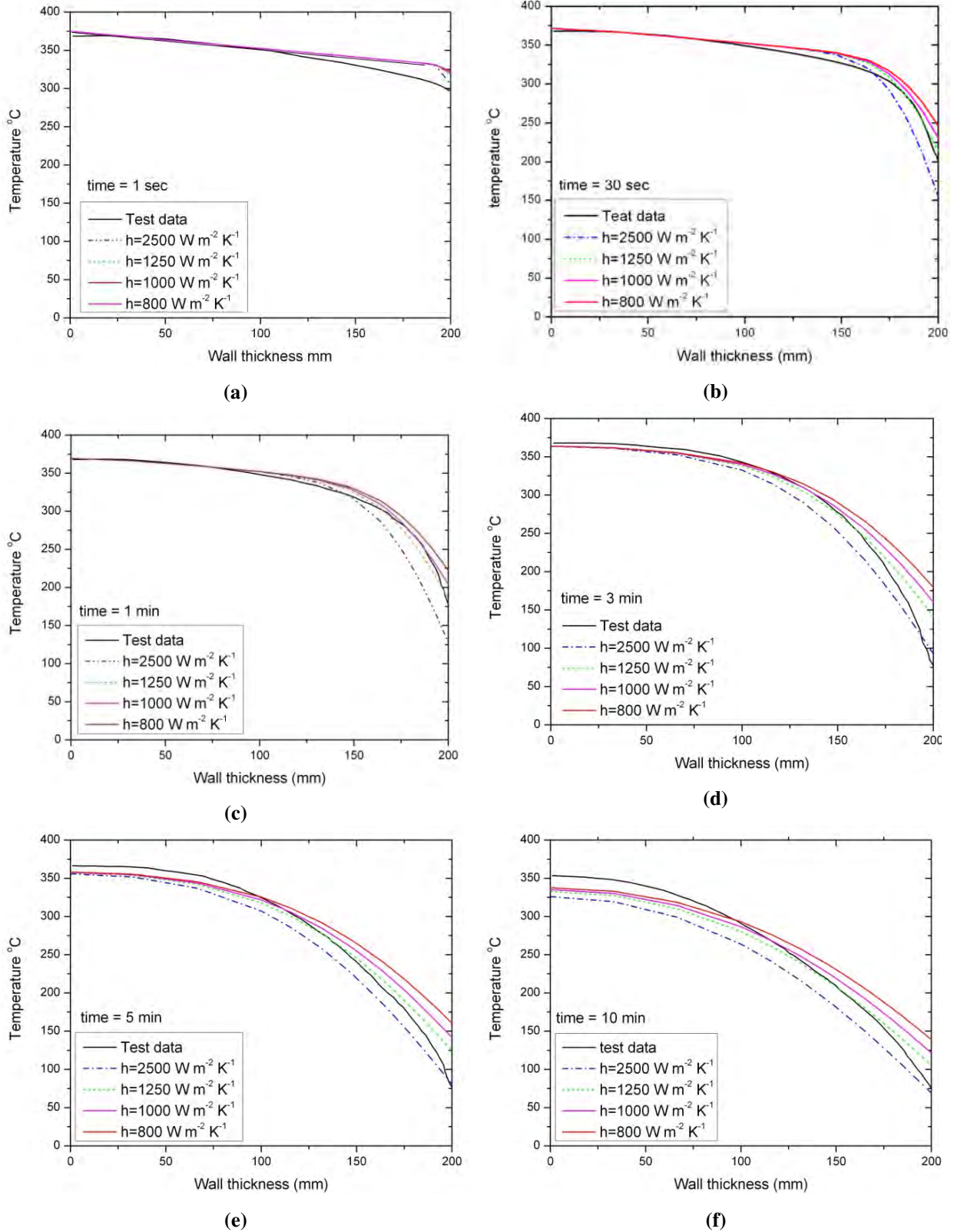


**Figure 7 (a-f) Thermal gradients across the thickness at different time intervals.**

## DETERMINATION OF HEAT TRANSFER COEFFICIENT FOR THERMAL SHOCK PROBLEM

An optimum value of heat transfer coefficient, which gives rise to similar thermal gradients that prevails in RPV wall during a PTS event, is essential for realistic simulation of the PTS event using cruciform specimen. Finite element analyses were carried out to obtain the suitable value of the heat transfer coefficient. A. Jovanovic et al. (1989) have reported an experimental study of a PTS event on a thick walled hollow cylinder having semi-elliptical crack in the inner surface. The cylinder is subjected to internal pressure and axial tension. Thickness of cylinder wall is 200 mm. Inner wall of the cylinder wall is maintained at 320°C and cooled rapidly by spraying the cold water. The temperature distribution along the thickness of the wall is recorded with time at different thickness levels. Jovanovic's experimental results are taken as reference for the PTS event. An FE model for cruciform specimen of same thickness as that of the cylinder wall in the experiment was analyzed. A static FE thermal analysis was first performed to get an initial temperature distribution in the core similar to that prevails in the cylinder wall at the beginning of the experiment. Figure 7(a) shows the initial temperature distribution in the core. Then four transient FE thermal analyses were performed by taking different values of heat transfer coefficients at the core surface (800, 1000, 1250 and 2500 Wm<sup>-2</sup>K<sup>-1</sup>). The temperature distribution at the centerline of the core for all the cases along with the Jovanovic's experimental data at different time intervals (30 seconds, 60 seconds, three minutes, five minutes, 10 minutes, and 15 minutes) are plotted in Figure 7(a-f). The curves corresponding to heat transfer coefficient 1250 Wm<sup>-2</sup>K<sup>-1</sup> are found to be in good agreement with the Jovanoiv's experimental data at different time intervals. This value of the heat transfer coefficient was used for pre-test thermal mechanical analyses of cruciform specimens.

**Table 4 The scheme of transient thermal analysis.**

Load step	Duration of Load step (seconds)	Time step size (second)	Total no. of sub-steps in a load step
1	1	0.05	20
2.	2	0.1	20
3.	26	0.5	52
4.	70	2	35
5.	900	10	90
6.	2000	20	100
total	2999		317

**Table 5 Results of thermo-mechanical analysis**

Specimen Name	Mechanical load				Mechanical and thermal combined load			
	Load (kN)	J-integral (kJ/m <sup>2</sup> )	COD (mm)	LLD (mm)	Jmax (kJ/m <sup>2</sup> )	Time (Second)	COD max (mm)	Time (second)
CR21NOC	1072.9	15.66	0.177	1.36	43.08	350	0.336	92
CR10	1401.3	339.53	1.07	34.8	443.36	609	1.337	229
CR11	1855.6	322.63	0.996	38.73	443.75	750	1.34	590
CR21	1820.32	310.19	0.961	53	406.86	560	1.1911	230

## THERMO MECHANICAL ANALYSES

Under pressurized thermal shock loading, RPV wall is subjected two types of stresses: first biaxial stresses, which arise due the application of pressure and second thermal stresses, which arise due to the presence of thermal gradients in the wall of a RPV. Biaxial stresses are produced in core of cruciform by application of bending load on the cruciform specimen and Thermal stresses are induced in the specimen by heating it to 300°C and then cooling the specimen using spray of water at room temperature. To analyze a simulated pressurized thermal shock problem using FEM, sequentially coupled

physics analysis approach was used. A brief description of the method adapted for such analysis for a specimen is as follows:

A transient thermal analysis was performed on a specimen for 3000 second. The description of load steps is shown in the Table 4. In this analysis an initial uniform temperature of 300°C was applied on the specimen and then it was allowed to cool through the core surface area by using a heat transfer coefficient of 1250 Wm<sup>-2</sup>K<sup>-1</sup> and ambient temperature 27°C. Typical temperature distributions along the thickness of the core of specimen at different time intervals are shown in Figure 8. Results (temperature distribution in the specimen at various time steps) of this analysis were saved for thermal structural analyses. After transient thermal analysis, a structural analysis was performed, where a bending load was applied on the specimen through the loading ram in load control manner. Then a series of thermal structural analyses were performed by taking temperature inputs from the results at various time steps of the previous transient thermal analysis.

Results of the coupled thermal mechanical finite element analyses for all the cruciform specimens are summarized in Table 4 and variations of fracture parameters such as J-integral, COD and LLD with time are shown in Figures 10 to 14. Maximum value of J-integral is reaching at 350 seconds for specimen CR21NOC and J-integral reaching to its peak value for specimen CR11 is 750 seconds.

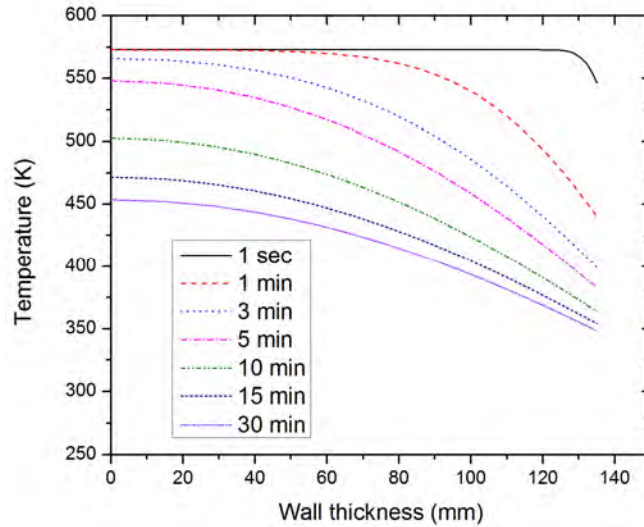


Figure 8 Typical temperature distributions across the thickness at the center of specimen core at different time intervals.

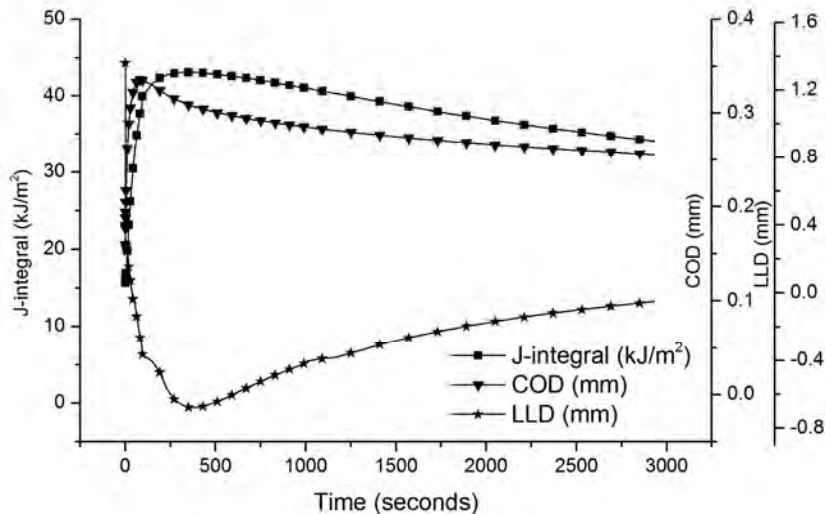


Figure 9 Variation of fracture parameters for specimen CR21NOC



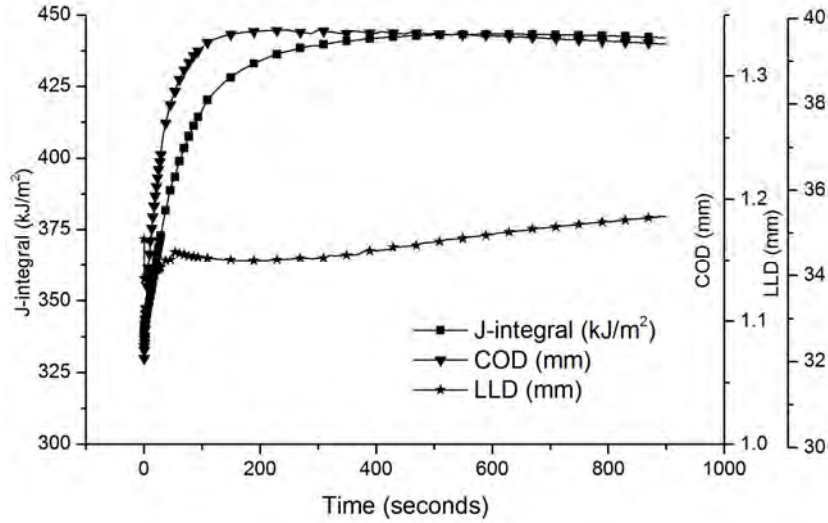


Figure 10 Variation of fracture parameters for specimen CR10

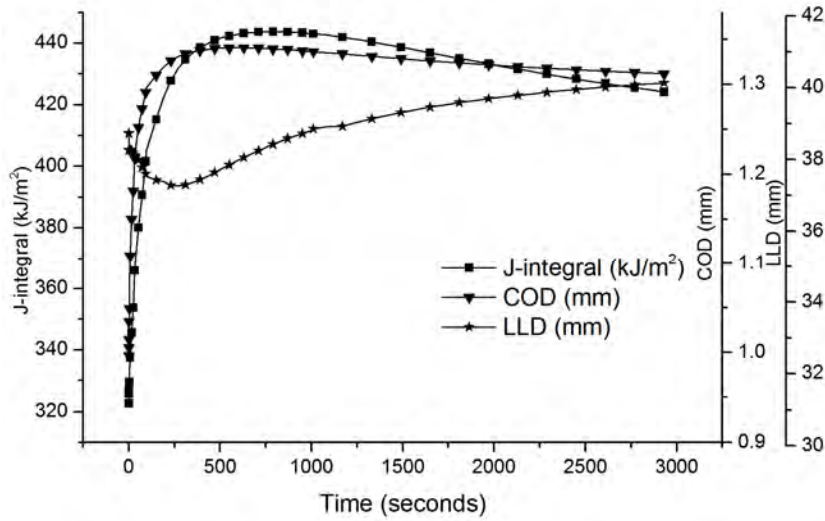


Figure 11 Variation of fracture parameters for specimen CR11

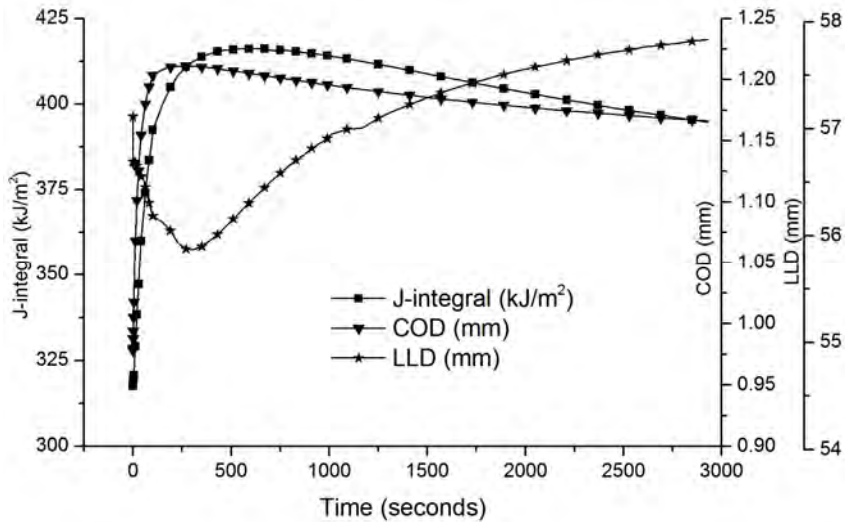


Figure 12 Variation of fracture parameters for specimen CR21

## CONCLUSIONS

Thermo-mechanical finite element analyses of four cruciform specimens were carried out as a part of pre-test calculations. These specimens were designed for carrying out simulated pressurized thermal shock test. One of the specimens, CR21NOC, was designed to simulate the actual operating conditions that prevail in an RPV. Crack driving force (J-integral) for the specimen CR21NOC remains under  $50 \text{ kJ/m}^2$  throughout the thermal transient, which is considerably less than the fracture toughness value of 20MnMoNi55 ( $\sim 300 \text{ kJ/m}^2$ ), hence no crack growth is expected during experiment. Remaining three specimens were designed to produce different biaxial stress ratios 1:0, 2:1 and 1:1. These three specimens were loaded till the onset of the crack-growth. Crack growth is expected in these cases as the crack driving force is exceeding the fracture toughness of the material.

## REFERENCES

- Jovanovic A., Sauter A. and Lucia A. C. Some current issues in the PTS research. Nucl. Eng. Des. 112 (1989) 259-278
- KTA SAFETY STANDARD Components of the Reactor Coolant Pressure Boundary of Light Water Reactors; Part 1: Materials and Product Forms KTA 3201.1 June 1998
- McAfee W. J., Brass B. R., Bryson J. W. Pennell W. E. Biaxial loading effects on fracture toughness of reactor pressure vessel steel. NUREG/CR-6273 (1995).
- McAfee W. J., Bryson J. W. Test and analysis of unclad finite-length flaw cruciform specimens. USNRC Report NUREG/CR-4219 (ORNL/TM9593/V12&NI), 1996:25-31
- Pennell W. E., Corwin W. R. Reactor pressure vessel Structural integrity research. Nucl. Eng DES, 1995; 157:159-175
- Schlapfer H.W., Barbezat G. and Borel M.O. Mat.-wiss. u. Werkstofftech. 21, 221-229 (1990)